

Blood pressure distribution in micro-vascular networks

Romain GUIBERT^{1,2,3,4,*}, Caroline FONTA^{3,4}, Franck PLOURABOUE^{1,2}

* Corresponding author: Tel.: +33 (0) 5 61 28 58 87; Fax: +33 (0) 5 61 28 58 99; Email: guibert@imft.fr

1: Université de Toulouse ; INPT, UPS ; IMFT (Institut de Mécanique des Fluides de Toulouse) ;
Allée Camille Soula, F-31400 Toulouse, France

2: CNRS ; IMFT ; F-31400 Toulouse, France

3: Université de Toulouse ; UPS ; Centre de Recherche Cerveau et Cognition ; France

4: CNRS ; CerCo ; F-31400 Toulouse, France

Abstract: Blood rheology is complex and non-linear. The effective viscosity variations are important due to red blood cells packing inside capillaries, the so-called Fåhræus-Lindquist effect, whilst concomitantly phase segregation appears in bifurcations. We have performed direct numerical simulations of different non-linear rheological models of the blood on realistic three-dimensional micro-vascular networks. These simulations point out two significant results. First, various rheological models lead to very similar pressure distributions over the whole range of physiologically relevant hematocrits. Secondly, different models for phase segregation lead to very distinct hematocrit distributions in the micro-vascular network. Moreover, for all the investigated rheological models, the hematocrit distribution very weakly affects the pressure distribution, when prescribing uniform pressure boundary conditions.

Keywords: Cerebral cortex, Micro-tomography, Micro-circulation, Blood rheology, Apparent viscosity, Fåhræus-Lindquist effect, Plasma skimming.

1. Introduction

Recent developments of imaging techniques allow a better understanding of biological systems, and more particularly intra-cortical micro-vascular networks. These networks have already been described qualitatively in the literature (Duvernoy *et al.*, 1981), but their topology and morphology are difficult to quantify. New imaging techniques permit high resolution three-dimensional acquisitions and accurate quantitative description of such networks (Plouraboué *et al.*, 2004).

The digital reconstruction of networks topology from high resolution images permits the modeling and simulation of micro-vascular blood flows. This modeling involves the coupling of a non-linear rheology with a very complex heterogeneous topology. This coupling has been mainly addressed on simple networks in the literature of the last twenty

years (Lee and Smith, 2008; Popel and Johnson, 2005).

A continuous approach is traditionally used to describe blood rheology. Discrete network models based on pressure drop computation between two successive bifurcations are used to compute the blood flow between two vascular junctions.

The purpose of our contribution is to provide a quantitative evaluation of blood pressure distribution within brain intra-cortical micro-vascular networks, and to evaluate the impact of different viscosity and plasma skimming models.

2. Acquisition and processing

The micro-vascular networks studied are extracted from primate cerebral cortex (marmosets). Sample preparation consists in injecting a contrast agent through the entire

vascular system. The injected tissue is treated using a specific preparation before resin inclusion. These samples are then imaged using synchrotron high resolution X-ray micro-tomography at the European Synchrotron Radiation Facility (Grenoble, France). Further details on the preparation and imaging have been described by Plouraboué *et al.* (2004).

This technique permits us to obtain ten millimeters cube scans over the entire depth of cortical gray matter with micron resolution. The volumes of data obtained are huge and difficult to handle in the form of gray-scale images. The very good contrast of these data allows to treat them by traditional image processing methods without loss of information.

The binarization is performed with an hysteresis thresholding method. Binary images are then filtered using erosion-dilation operators with a three-dimensional cubic structuring element to remove isolated islands of pixels, as well as pixels holes inside vessels. The image is then skeletonized to obtain a vectorized description of the network which is lightweight, easy to manipulate, and contains all the necessary information. Finally, a specific method which fills the gaps between the closest discontinuous vessels has been developed to recover the complete real network topology (Risser *et al.*, 2008; 2009).

3. Background about micro-circulation

3.1 Fåhræus and Fåhræus-Lindquist effects

Many studies have focused on blood rheology modeling whose specificities are mainly related to the presence of red blood cells and their ability to deform when they move into smallest vessels. These studies have shown that red blood cells rate flowing in a tube (tube hematocrit) is lower than the systemic hematocrit. This effect is called the Fåhræus

effect.

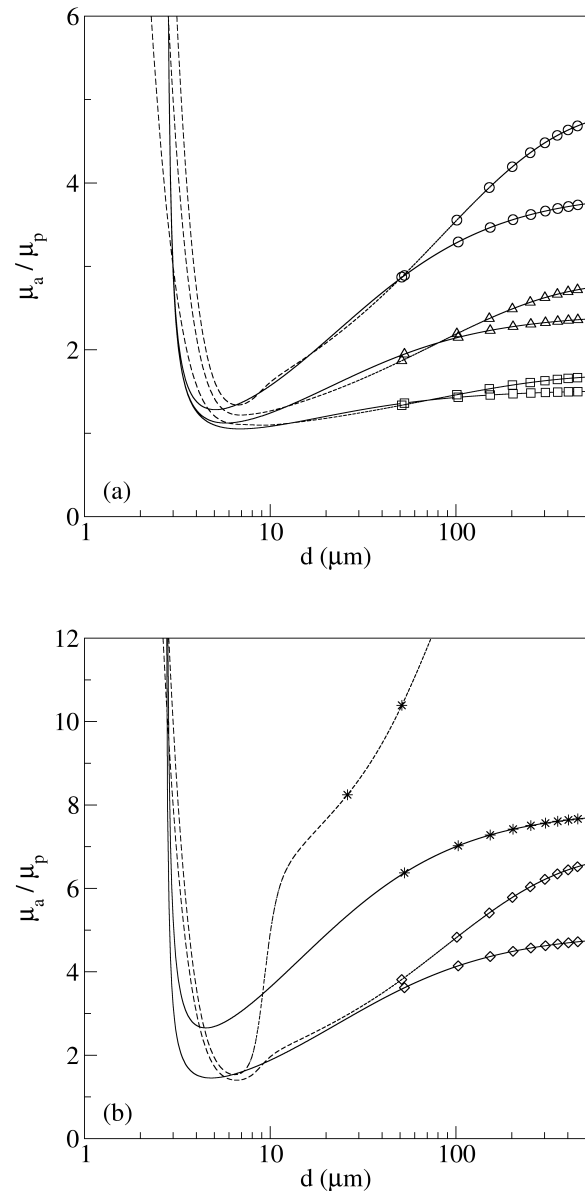


Figure 1. Relative apparent viscosity versus vessel diameter using Kiani and Hudetz (1991) (solid lines) and *in vitro* Pries *et al.* (1990) (dashed lines) models for different systemic hematocrit (a) $h = 0.2$ (square), $h = 0.4$ (triangle), $h = 0.6$ (circle) and (b) $h = 0.7$ (diamond), $h = 0.9$ (star).

Furthermore, when tube diameter reaches values comparable to capillary size, i.e. 5-10 μm , the apparent viscosity of blood decreases as the diameter value goes down. This remarkable phenomenon is the Fåhræus-Lindquist effect. It reflects the structure of the two-phase flow which minimized the viscous dissipation. Red blood cells concentrate at the

vessels center, the plasma lubricates the flow, so that the apparent viscosity of blood decreases. This behavior saturates when red blood cells can not more deform.

The *in vitro* viscosity models proposed by Pries *et al.* (1990) and Kiani and Hudetz (1991) are based on systemic hematocrit that we note h . These two models are illustrated in figures 1a,b. They exhibit very similar behaviors within the relevant physiological hematocrit range $0 < h < 0.6$ (figure 1a). However, the viscosity minimum is achieved at a slightly different diameter for both models. The behavior of the two models significantly differs in the hematocrit range $0.6 < h < 1$ (figure 1b).

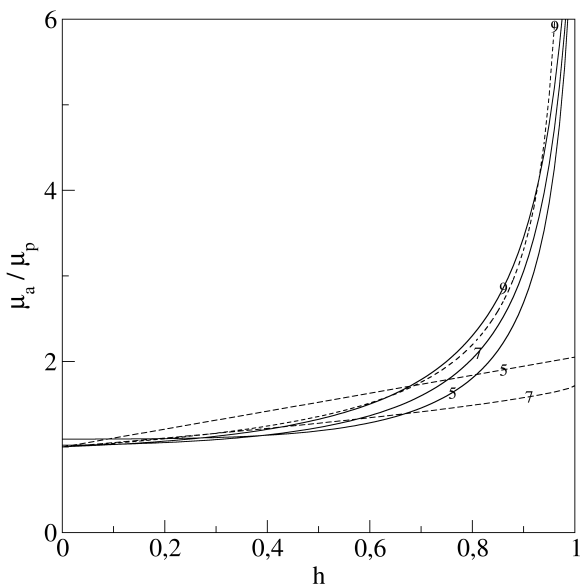


Figure 2. Relative apparent viscosity function of hematocrit using Kiani and Hudetz (solid lines) and *in vitro* Pries *et al.* (dashed lines) models for different tube diameters $d = 5, 7, 9 \mu\text{m}$.

It is also interesting to visualize the apparent viscosity variations versus the hematocrit. Figure 2 illustrates the weak influence of the hematocrit on the *in vitro* apparent viscosity when its value is lower than 0.6. More precisely, we observe less than 20% variations for hematocrits in the range $0 < h < 0.6$. This is not the case for *in vivo* viscosity laws which present a more important dependence on the hematocrit as illustrated in figure 3.

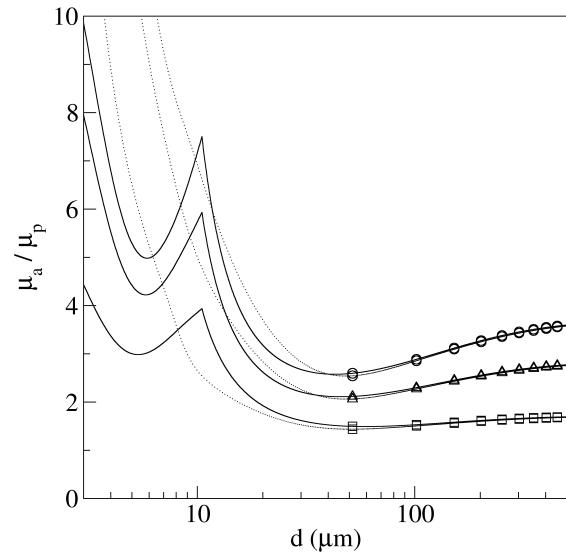


Figure 3. Relative apparent viscosity versus vessel diameter using Pries *et al.* (1994) (dotted lines) and Pries and Secomb (2005) (continuous lines) *in vivo* viscosity laws for different systemic hematocrit: $h = 0.2$ (square), $h = 0.4$ (triangle), $h = 0.6$ (circle).

Pries *et al.* (1994) then Pries and Secomb (2005) have also proposed several forms of *in vivo* viscosity laws. These laws have been established by minimizing the difference between experimental *in vivo* measurements and direct simulations. The viscosity values are higher than the ones predicted by *in vitro* laws, due to the presence of endothelial surface layer.

Using these different laws, the respective contributions of the network structure (associated with the vessel diameter) and the blood rheology on the blood pressure distribution may therefore be quite different. Further complete pressure simulations will be necessary to investigate this qualitative observation about the models of rheology.

3.2 Plasma skimming

The phase separation is characterized by a non-uniform distribution of red blood cells in the branches of a bifurcation. Again, different non-linear empirical models have been proposed by Dellimore *et al.* (1983) and Pries *et al.* (1990, 1994) to describe *in vitro* and *in*

vivo experimental observations.

The first model (Dellimore *et al.*, 1983) only considers the blood flow influence on the hematocrit distribution in mother/daughter branches of a junction. However, the more complex model proposed by Pries *et al.* (1990, 1994) and Pries and Secomb (2005), also takes into account the influence of flow distributions, input hematocrit and diameters. These models are based on a local approach of plasma skimming phenomenon and require local knowledge of the flow direction. They can only be used when the flow is directed from the mother branch (indexed m) into the daughter branches (indexed α and β). In the following we call “incoming bifurcations” those for which there are one inflow and two outflows. We also call “outgoing bifurcations” those for which there are two inflows and one outgoing. Only red blood cells flow conservation is applied for this last one.

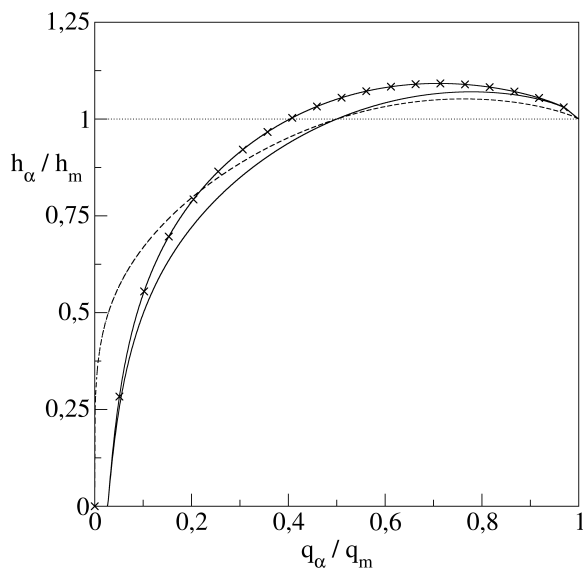


Figure 4. Hematocrit ratio versus flow ratio using plasma skimming models of Dellimore *et al.* (dashed lines) and Pries and Secomb (2005) (continuous lines) for bifurcations characterized by $d_m = d_\alpha = d_\beta = 20 \mu\text{m}$ and $d_m = d_\beta = 20 \mu\text{m}$, $d_\alpha = 15 \mu\text{m}$ (cross).

Figure 4 illustrates hematocrit ratio predicted by these models for incoming bifurcations. It is important to note that both models can lead

to hematocrit ratio higher than unity for a particular range of flow ratio between mother and daughter vessels and for some diameters. Therefore, in certain circumstances arising in complex networks these models can predict daughter hematocrit larger than one when mother hematocrits are high, which is unacceptable from the modeling point of view. The version proposed by Pries and Secomb (2005) is adjusted to contain the hematocrit rates.

Mathematical details of the different models mentioned above can be found within the provided references.

4. Hydrodynamic model

The brain micro-vessels have the property to be highly elongated so that the diameter/length ratio is about 1/10. The lubrication approximation can be profitably used to assess the induced pressure drop in tube having diameter variations.

From the asymptotic analysis of the Stokes equation, it is possible to find a Poiseuille's law, which characterizes the flow in a tube. The flow rate q is proportional to the longitudinal pressure gradient ∇p , *i.e.*

$$q = \frac{\pi d^4}{128 \mu_a} \nabla p. \quad (1)$$

The coefficient of proportionality which connects q and ∇p known as the hydraulic conductance shows a strong dependence with the fourth power of the local diameter. However it shows a smaller dependence with rheological properties of the fluid as it is only inversely proportional to the apparent viscosity. By integrating equation (1) between two successive bifurcations, we get a pressure drop relation, which connects local pressures at junctions and takes into account the apparent viscosity of the fluid as well as the local vessel diameter variations. The above mentioned viscosity models are used to evaluate the apparent viscosity.

Such integrated pressure drop between two successive bifurcations neglects the influence of the possibly complex flow arising in the vicinity of each bifurcation. Nevertheless it is expected that the contribution of these localized complex hydrodynamical effects is of order of the diameter/length ratio which is about 1/10 in physiological networks. Such effects would bring rather small corrections to the pressure drop and can then be safely discarded.

To determine the limit of the quasi-static pressure distribution in these networks, we write the flow conservation at each node of the network as:

$$\sum_i q_i = 0 . \quad (2)$$

The equation (2) leads to a linear system applied to pressure nodes. It can be solved using a direct method adapted to sparse matrices, taking into account boundary conditions imposed on border pressure nodes. Using a dimensionless form of these equations, we impose $p=1$ for input nodes and $p=0$ for output ones. Solving the pressure problem is in fact the first step of an iterative process proposed by Pries *et al.* (1990).

The second step consists in the resolution of the hematocrit mass conservation written at each bifurcation. Hematocrit changes resulting from phase separation require a second conservation law for all bifurcations:

$$\sum_i h_i q_i = 0 . \quad (3)$$

The relation (3) is locally applied. In the case of incoming bifurcations, equation (3) is applied through plasma skimming local models. In practice, using Pries *et al.* model, nodes have to be ordered to know the mother hematocrit.

The hematocrit field calculated from phase separation models is then used to solve the

pressure field at next iteration. The convergence of this iterative procedure may be difficult. In some cases, over-relaxation is used to facilitate the convergence.

5. Results

To study the impact of viscosity and phase separation models, we evaluate pressure and hematocrit distribution in a real intra-cortical micro-vascular network of 1,5 mm³. Figures 5 and 6 show the complex structure of this network located below the pial mater (under the brain surface). One can distinguish cortical columns, or perforating arteries, which pass through the entire volume, and feed a heterogeneous capillary bed. This network consists of a single connected component, and includes 3700 segments of vessels. The diameters distribution of this network is centered around a diameter of 10 μm. The quasi-static pressure and hematocrit distribution, colored on these same figures, are calculated using the models proposed by Pries and co-workers.

We then consider four configurations C_i of viscosity law and phase separation models. At each node of the network we compute the pressure given by each configuration p^C . For two configurations C_1 and C_2 we then compare the average relative difference between the pressure at each node i :

$$E = \frac{1}{N} \max \left(\sum_i \frac{|p_i^{C_1} - p_i^{C_2}|}{p_i^{C_1}}, \sum_i \frac{|p_i^{C_1} - p_i^{C_2}|}{p_i^{C_2}} \right) . \quad (4)$$

We observe that this relative pressure difference E does not exceed 3,20 %, when comparing different viscosity laws and plasma skimming models as summarized in table 1. Moreover, we compare these pressure distributions to the ones obtained using an uniform hematocrit distribution, and we also observe weak differences (table 2).

Figures 7 and 8 show the pressure and hematocrit histograms obtained using the *in*

in vivo viscosity law proposed by Pries and Secomb (2005) or Kiani and Hudetz (1991) coupled with the two plasma skimming models used above. Differences on pressure distribution are minimal for a given effective rheology viscosity law. The distribution of hematocrits in the network varies widely from one model to another, but this strong difference has a very low impact on the pressure distribution.

	V: Pries / Secomb S: Dellimore <i>et al.</i>	V: Kiani / Hudetz S: Dellimore <i>et al.</i>
V: Pries / Secomb S: Pries / Secomb	0.23 %	3.20 %
V: Kiani / Hudetz S: Pries / Secomb	3.12 %	0.27 %

Table 1. Average relative pressure difference E given in (4) for different couples of viscosity laws (indicated by V) and phase separation (indicated by S) models.

	V: Pries / Secomb	V: Kiani / Hudetz
S: Pries / Secomb	0.42 %	0.55 %
S: Dellimore <i>et al.</i>	0.26 %	0.40 %

Table 2. Analysis of the impact of plasma skimming models on the pressure distribution. We compare the pressure distribution in configuration V/S with the one resulting from a uniform hematocrit distribution associated with the same viscosity law V by evaluating the average relative difference E given in (4).

6. Conclusion

Different continuous models have been proposed to describe blood rheology in the literature and so the more for plasma skimming effect. We have computed numerically the flow distribution given by these models in the context of real three-dimensional micro-vascular networks. Our calculations have revealed some salient properties of confined blood rheology. We observe that the impact of phase segregation models is indeed very weak on the pressure distribution. The complex structure of the hematocrit inside heterogeneous networks has

a negligible impact on pressure distribution. This result is even observed when considering *in vivo* viscosity laws which are more sensitive to the coupling between hematocrit and effective viscosity. Variations of vessel diameter are essentially responsible for the pressure distribution configuration. These observations are to be related to the drastic dependence of the local conductance (1) on the diameter. This observation leads to the conclusion that the blood pressure predictions may be a reliable quantity to compute because it weakly depends on the considered models, all the more so on the plasma skimming ones.

Our results also suggest that the modeling of blood rheology can ignore the plasma skimming phenomenon without affecting the pressure distribution by more than 3.5%. Given the possible weakness of these phase separation models, the numerical difficulties associated with their resolution, as well as the high disparity of their impact, this result opens interesting prospects for the simplification and the reliability of micro-vascular pressure computation. This result should nevertheless be tempered by the possible influence of the applied boundary conditions in the present study. Moreover, it is important to stress that even if the phase-segregation effect has a minor influence on the pressure distribution, it is of major importance for transport issues such as oxygen distribution in micro-vascular networks.

Acknowledgments

The authors thank the referees for their fruitful comments to this study. The research was supported by GDR n° 2760 - Biomécanique des fluides et des transferts - Interaction fluide/structure biologique, the ASUPS A03 and A05 of Paul Sabatier University, Toulouse, France and the ANR project ANR-06-BLAN-0238-01.

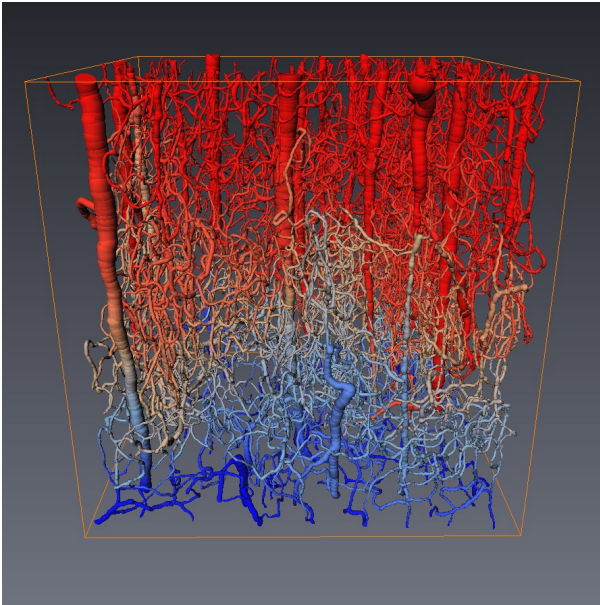


Figure 5. Pressure distribution using Pries *et al.* *in vivo* viscosity and plasma skimming models. Systemic hematocrit $h = 0.45$. Decreasing colour-coded representation from red to blue.

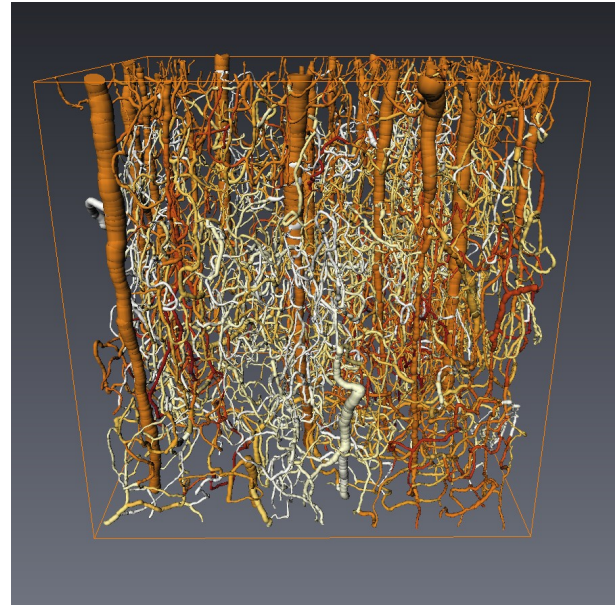


Figure 6. Hematocrit distribution using Pries *et al.* *in vivo* viscosity and plasma skimming models. Systemic hematocrit $h = 0.45$. Decreasing colour-coded representation from dark to light.

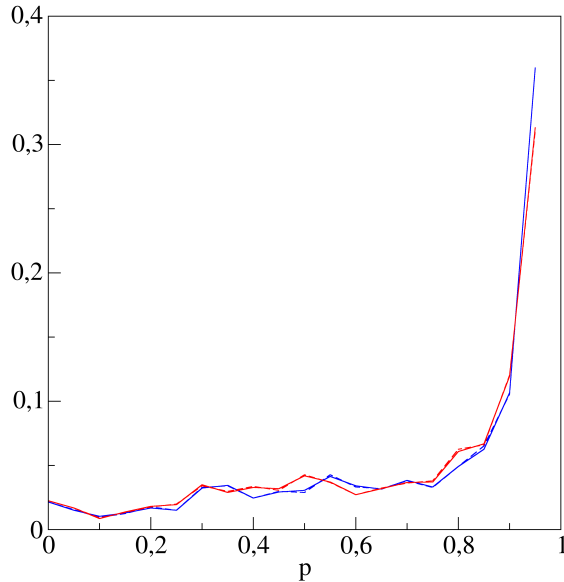


Figure 7. Node pressure histogram using *in vivo* Pries *et al.* (blue) or Kiani and Hudezt (red) viscosity laws, and Pries *et al.* (continuous lines) or Dellimore *et al.* (dashed lines) phase separation models. Pressure boundary conditions are not plotted. Continuous and dashed lines are superimposed.

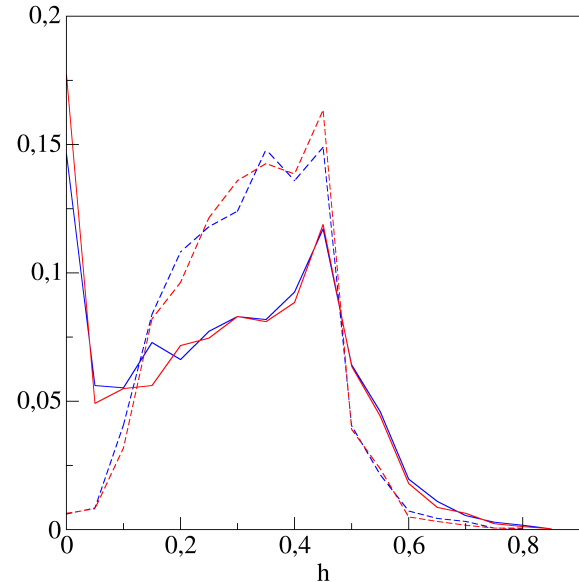


Figure 8. Segment hematocrit histogram using *in vivo* Pries *et al.* (blue) or Kiani and Hudezt (red) viscosity laws, and Pries *et al.* (continuous lines) or Dellimore *et al.* (dashed lines) phase separation models. Inlet hematocrit values are not plotted.

References

Dellimore, J. W., Dunlop, M. J., Canham, P. B., 1983. Ratio of cells and plasma in blood flowing past branches in small plastic channels. *Am. J. Physiol. Heart Circ. Physiol.* 244, 635–643.

Duvernoy, H. M., Delon, S., Vannson, J. L., 1981. Cortical blood vessels of the human brain. *Brain Res. Bull.* 7, 519–579.

Kiani, M. F., Hudetz, A. G, 1991. A semi-empirical model of apparent blood viscosity as a function of vessel diameter and discharge hematocrit. *Biorheology* 28, 65–73.

Lee, J., Smith, N. P., 2008. Theoretical modeling in hemodynamics of microcirculation. *Microcirculation* 15, 699–714.

Plouraboué, F., Clotens, P., Fonta, C., Steyer, A., Lauwers, F., Marc-Vergnes, J.-P., 2004. X-ray high-resolution vascular network imaging. *J. Microsc.* 215, 139–148.

Popel, A. S., Johnson, P. C., 2005. Microcirculation and hemorheology. *Annu. Rev. Fluid Mech.* 37, 43–69.

Pries, A. R., Secomb, T. W., 2005. Microvascular blood viscosity in vivo and the endothelial surface layer. *Am. J. Physiol. Heart Circ. Physiol.* 289, 2657–2664.

Pries, A. R., Secomb, T. W., Gaehtgens, P., Gross, J. F, 1990. Blood flow in microvascular networks. Experiments and simulation. *Circ. Res.* 67, 826–834.

Pries, A. R., Secomb, T. W., Gessner, T., Sperandio, M. B., Gross, J. F, Gaehtgens, P., 1994. Resistance to blood flow in microvessels in vivo. *Circ. Res.* 67, 826–834.

Risser, L., Plouraboué, F., Cloetens, P., Fonta, C., 2009, A 3D investigation shows that

angiogenesis in primate cerebral cortex mainly occurs at capillary level. *Int. J. Dev. Neurosci.* 27, 185-196.

Risser, L., Plouraboué, F., Descombes, X., 2008. Gap filling of 3D micro-vascular networks by tensor voting. *J. Cereb. Blood Flow Metab.* 27, 674–687.